UC San Diego
UC San Diego Previously Published Works

Title

Comparative analysis of mouse and human placentae across gestation reveals species-specific regulators of placental development

Permalink

Journal

ISSN

Authors

Soncin, Francesca
Khater, Marwa
To, Cuong
et al.

Publication Date

DOI

Comparative analysis of mouse and human placentae across gestation reveals species-specific regulators of placental development

Francesca Soncin[1,3], **Marwa Khater**[2,3], **Cuong To**[2,3], **Donald Pizzo**[1], **Omar Farah**[1,3], **Anna Wakeland**[1,3], **Kanaga Arul Nambi Rajan**[1,3], **Katharine K. Nelson**[1,3], **Ching-Wen Chang**[1,3], **Matteo Moretto-Zita**[1,3], **David R. Natale**[2], **Louise C. Laurent**[2,3,*] and **Mana M. Parast**[1,3,*]

ABSTRACT

An increasing body of evidence points to significant spatio-temporal differences in early placental development between mouse and human, but a detailed comparison of placentae in these two species is missing. We set out to compare placentae from both species across gestation, with a focus on trophoblast progenitor markers. We found that CDX2 and ELF5, but not EOMES, are expressed in early post-implantation trophoblast subpopulations in both species. Genome-wide expression profiling of mouse and human placentae revealed clusters of genes with distinct co-expression patterns across gestation. Overall, there was a closer fit between patterns observed in the placentae when the inter-species comparison was restricted to human placentae through gestational week 16 (thus, excluding full-term samples), suggesting that the developmental timeline in mouse runs parallel to the first half of human placental development. In addition, we identified VGLL1 as a human-specific marker of proliferative cytotrophoblast, where it is co-expressed with the transcription factor TEAD4. As TEAD4 is involved in trophectoderm specification in the mouse, we posit a regulatory role for VGLL1 in early events during human placental development.

KEY WORDS: Placenta, Trophoblast stem cells, Placental development, Cytotrophoblast, Placental progenitors, Comparative study

INTRODUCTION

The placenta is a temporary organ dedicated to supporting fetal growth during gestation by providing an interface for nutrient and gas exchange, as well as hormones that are essential for development. Although we have some knowledge of human placental development and function, particularly from later gestational stages, its early development during the peri-implantation period is poorly understood. Abnormal trophoblast differentiation early in gestation is considered the root cause of many placenta-associated pregnancy complications, such as miscarriage, preeclampsia and intra-uterine growth restriction, and

clarification of these mechanisms may point to novel interventional approaches for such disorders (Cuffe et al., 2017; Norwitz, 2006; Steegers et al., 2010).

Study of early human placental development is hampered by practical and ethical issues. Therefore, both animal and *in vitro* (cell culture) models are routinely used to probe trophoblast lineage specification and function. Rodents, and in particular mice, have been the primary models used to study placental development. Importantly, both mouse and human placentae are discoid in shape and show a hemochorial gas-nutrient exchange interface. However, fundamental differences exist between rodents and humans, including gestational length, litter size, and the component trophoblast cell types and their organization within the placenta (Soncin et al., 2015). Recently, significant differences have been identified between mouse and human blastocyst-stage embryos (Blakeley et al., 2015; Deglincerti et al., 2016; Niakan and Eggan, 2013; Shahbazi et al., 2016). Specifically, whereas in mouse blastocysts, the inner cell mass (ICM) and trophectoderm (TE) compartments are clearly marked by mutually exclusive expression of POU5F1/OCT4 and CDX2, there is co-expression of these two markers in human TE (Niakan and Eggan, 2013). In addition, EOMES and ELF5 are absent from pre-implantation human embryos (Blakeley et al., 2015), although ELF5 has been found, along with CDX2, in a subset of the cytotrophoblast (trophoblast progenitor cells) in early post-implantation placentae (Hemberger et al., 2010). Conversely, GATA3 has been identified as a consistent marker of trophectoderm and the early cytotrophoblast (Deglincerti et al., 2016; Lee et al., 2016). These data, along with the inability to derive human trophoblast stem cells (TSC) from pre-implantation blastocyst-stage embryos (Kunath et al., 2014), suggest at least a spatio-temporal difference between early events during TE establishment and differentiation in the two species. Nevertheless, the many advantages of transgenic mouse models, including the ability to evaluate the contribution of specific genes to both placental and fetal development, make the mouse system an indispensable tool for identification of pathways involved in trophoblast lineage specification and differentiation, and placental development.

To better understand the strengths and limitations of the mouse system, we set out to compare mouse and human placental development across gestation, from early in the post-implantation period to full term, with a focus on studying in detail the cytotrophoblast of the early post-implantation human placenta. We started by evaluating the mouse TSC markers CDX2, ELF5 and EOMES in the human placenta by immunohistochemistry and/or a highly sensitive *in situ* hybridization method. These three factors regulate a transcriptional program involved in maintenance and

[1]Department of Pathology, University of California San Diego, La Jolla, CA 92093, USA. [2]Department of Reproductive Medicine, University of California San Diego, La Jolla, CA 92093, USA. [3]Sanford Consortium for Regenerative Medicine, La Jolla, CA, 92037, USA.

*Authors for correspondence (llaurent@ucsd.edu; mparast@ucsd.edu)

F.S., 0000-0002-7423-9167; O.F., 0000-0003-4446-5478; A.W., 0000-0002-9442-8029; K.A., 0000-0001-6580-7524; M.M., 0000-0003-3846-7653; M.M.P., 0000-0001-5963-2246

expansion of the TSC population in mice (Senner and Hemberger, 2010), but their expression in the human placenta has not been characterized in detail. In addition, we compared the transcriptomes of placentae from these two species across gestation using genome-wide microarray-based gene expression profiling. As human placental villi contain a continuous layer of cytotrophoblast in early gestation, which becomes discontinuous and eventually sparse in late gestation, we reasoned that differential expression analysis comparing early and late gestation placentae should identify at least some of the genes that are specific to this trophoblast progenitor cell type, with expression of such genes decreasing across gestation. In addition, comparison of trajectories of co-expressed clusters of genes between mouse and human suggests that mouse placental development across gestation corresponds to the first half of gestation in the human placenta. In addition, although there was little overlap in the expression patterns of specific genes during this period of placental development in mouse and human, we found at least a partial overlap in enriched biological process terms associated with up- and downregulated genes over gestation. Finally, we created species-specific networks of co-regulated transcription factors, allowing us to identify common and species-specific 'master' regulator genes important for early placental development. Among these, we identified and characterized a member of the vestigial-like family of transcriptional co-factors as a novel human-specific cytotrophoblast marker.

RESULTS
### Stem cell markers in human placentae across gestation
We determined spatio-temporal distribution of three established mouse trophoblast stem/progenitor markers, CDX2, ELF5 and EOMES, in the human placenta throughout gestation. We have previously shown using immunohistochemistry that CDX2 expression in early gestation human placentae localizes to a subset of cytotrophoblast (CTB) cells (Horii et al., 2016). On further inspection, we noted that, within early gestation, placentae (5-8 weeks gestational age), CDX2$^+$ CTB cells were most abundant near the chorionic plate (CP), with the percentage of CDX2$^+$ CTB cells decreasing as villi approach the basal plate (BP) (Fig. 1A,Bi,

ii); no CDX2 was detected in the CTB of anchoring villi (Fig. 1Biii). CDX2 expression was also absent from the syncytiotrophoblast (STB, Fig. 1Ci,ii) and extravillous trophoblast (EVT, Fig. 1C iii) at all gestational ages.

Because immunohistochemistry using multiple antibodies against ELF5 and EOMES resulted in only non-specific cytoplasmic staining (data not shown), we turned to a novel highly sensitive *in situ* hybridization technique for evaluation of these two transcription factors. Using this method, we detected *ELF5* mRNA primarily in the CTB and proximal cell column EVT of early gestation placentae (Fig. 2A), with lower levels detected in the STB (Fig. 2A) and more mature EVT [in distal cell columns of early, and basal plates of late, gestation placentae (data not shown)]. Expression decreased dramatically in the second trimester and was restricted to the CTB (Fig. 2B); by full term, the CTB contained only rare copies of the transcripts of this marker (not shown). Using the same method, *EOMES* mRNA expression was found to be absent from all stages of human placenta analyzed. *EOMES*-specific probes were validated in several positive control tissues, including human tonsils and various types of human cancers, namely breast, lung and cervical tumors (Fig. S1 and data not shown).

Genome-wide RNA profiling
To broaden the scope of our comparative study of mouse and human placentae across gestation beyond a handful of markers, we performed genome-wide microarray-based RNA profiling and compared gene expression both across time and between species, using 54 normal human placenta samples collected between 4 and 39 weeks gestational age, and 54 mouse placenta samples collected between E7.5 and E18.5 gestational stages. For both species, we used principal component analysis (PCA) to identify and remove potential outliers. After filtering the gene lists to retain transcripts with variance cutoff 0.02 in Qlucore, PCA1 showed a correlation with gestational age for both human and mouse placenta (Fig. S2A, C). Hierarchical clustering using this minimally filtered gene list revealed that mouse placental samples formed distinct clusters according to day of gestation (Fig. S2A). For the mouse dataset, differential expression analysis comparing the samples according to
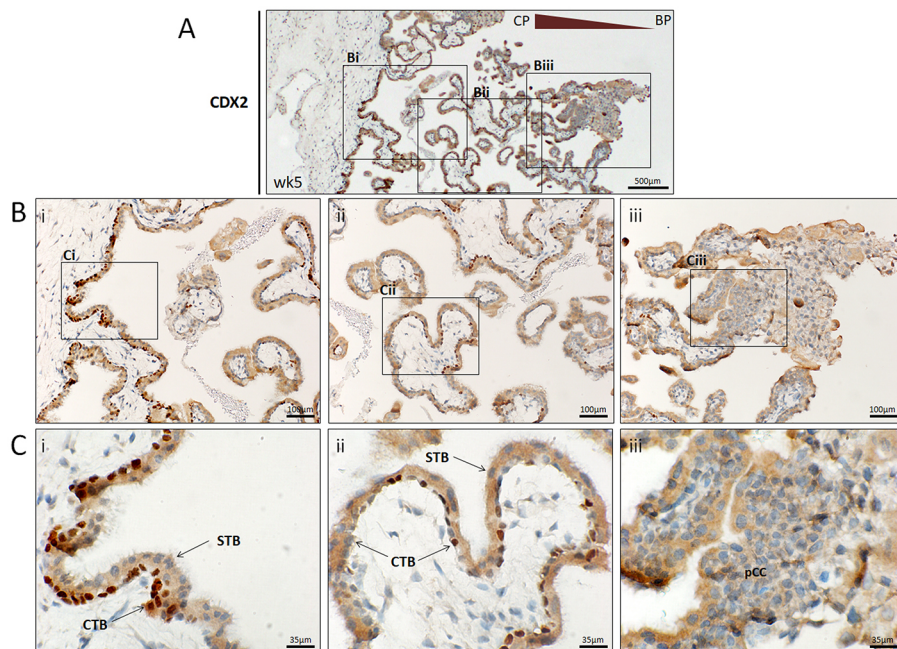
Fig. 1. CDX2 is highly expressed in a subpopulation of human villous cytotrophoblast near the chorionic plate. Immunohistochemistry for CDX2 in early post-implantation human placenta (week 5). (A-C) Nuclear expression was noted in a subpopulation of the villous CTB, concentrated near the chorionic plate (CP), and became less frequent towards the basal plate (BP). No nuclear staining was noted in the syncytiotrophoblast (STB; Ci,ii) or proximal cell column trophoblasts (pCC; Ciii). Squares in A,B indicate the areas magnified in B,C, respectively. CTB, cytotrophoblast; pCC, proximal cell column trophoblast; STB, syncytiotrophoblast; wk, week.
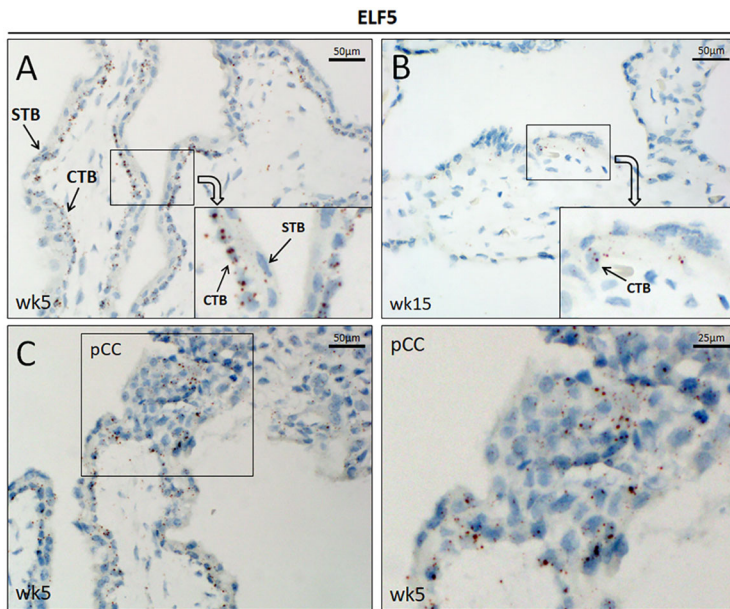
Fig. 2. ELF5 is expressed in both villous cytotrophoblast and proximal cell column trophoblast in early human placenta. *In situ* hybridization was performed using an ELF5-specific probe, showing a wider expression pattern in first trimester human placentae than previously reported. (A) ELF5 expression in first trimester villous samples was highest in the CTB. (B) By the second trimester, ELF5 expression was decreased and became restricted to the CTB. (C) Expression of ELF5 in week 5 extravillous trophoblast located in the proximal cell columns (pCCs). In C, the right image is at twice the magnification of the left image; in A,B, the insets are at twice the magnification of the main image. CTB, cytotrophoblast; pCC, proximal cell column; STB, syncytiotrophoblast; wk, week.

day of gestation was then used to decrease the dimensionality of the dataset (q≤0.05 and FC≥2) to 2947 differentially expressed genes (DEGs) (Fig. 3A, Table S1). Five representative DEGs were randomly selected and their differential expression confirmed using qPCR (Fig. S2B).

The human placental samples were more variable, but also showed gestational age progression along PCA1 (Fig. S2C). However, hierarchical clustering did not separate these samples clearly according to the week of gestation (Fig. S2C). Term samples had a well-defined signature, as expected by the large temporal difference compared with the other samples. The rest of the samples displayed a general correlation with gestational age, with the earliest samples on the left and later samples on the right, but with frequent overlap in the distributions of samples from different timepoints. Therefore, we used hierarchical clustering to separate the samples into groups according to their gene expression patterns, rather than the clinically determined gestational age. The samples from weeks 8 and 12 showed a broad distribution in the PCA plot, and were therefore removed, along with previously identified outliers, narrowing down the sample set to 31 samples. The hierarchical clustering identified six groups (Fig. 3B): groups A and B included samples from weeks 4-5 and weeks 6-7, respectively; groups C and D each contained a combination of samples from weeks 9 to 11; and, finally, groups E and F represented second trimester and full-term samples, respectively. Differential expression analysis between these sample groups identified 1195 human placenta DEGs (Fig. 3B, Table S1). Five representative DEGs were randomly selected and their differential expression confirmed using qPCR (Fig. S2D).

Comparing the list of DEGs between the two species, we found 517 genes to be in common, representing only 18% of mouse and 43% of human DEGs (Fig. 3C). For each species, the DEGs displayed two main expression patterns across gestation, upregulation and downregulation, consisting of 35% and 48% of the common DEGs, respectively, with the remaining genes (~20%) showing other expression patterns (Fig. 3D, center pie chart). We subsequently investigated the common DEGs for direction of expression for the two main expression patterns, down- and upregulation across gestation (Fig. S3A,B). In this analysis, 129

genes showed parallel upregulation and 157 showed parallel downregulation across gestation in both species, with the remaining 231 having different patterns of expression (including 48 with completely opposing expression patterns) in mouse and human (Fig. 3D, side pie charts). To confirm that these observations reflected a true difference between mouse and human, and were not technical artifacts, we compared the DEGs from our mouse analysis with a similar but smaller dataset from Knox and Baker (2008). Applying the same differential expression thresholds, about 40% of DEGs were common to both mouse studies, of which over 96% showed comparable expression patterns across gestation (Fig. S3C, D). Moreover, the microarray data from human placentae confirmed CDX2 and ELF5 downregulation across gestation seen in the immunohistochemistry and *in situ* hybridization experiments, while the probe for EOMES did not pass the minimum signal threshold to be included in the analysis (Fig. S3E).

Next, we identified the enriched gene ontology (GO) terms in the Biological Process tree in the commonly up- (red) and down- (green) regulated genesets (Fig. 3E). Genes downregulated with gestation were enriched for regulation of the cell cycle and various DNA and cellular metabolic pathways. In contrast, genes upregulated with gestation were enriched for functions associated with cell differentiation, maturation and specialization. When we analyzed the GO terms associated with the species-specific differentially expressed genesets, we found modest overlaps in the enriched GO biological process terms (about 30%), despite the absence of common genes in the mouse and human lists (Fig. S4). Downregulated genes (Fig. S4A) were associated with cell cycle and protein synthesis, whereas upregulated genes (Fig. S4B) represented cell migration and cell/organ maturation, with a strong focus on blood vessel development and cell signaling activation/regulation.

To start unravelling the complexity of the biology during placental development across gestation, we applied the affinity propagation (AP) algorithm to each species dataset. For the mouse dataset, AP clustering of the 2947 DEGs yielded seven clusters of co-expressed genes (Fig. 4A, Table S1), showing specific patterns of expression across gestation. Three clusters (#2, #3 and #7) showed a trend of downregulation across gestation, albeit with
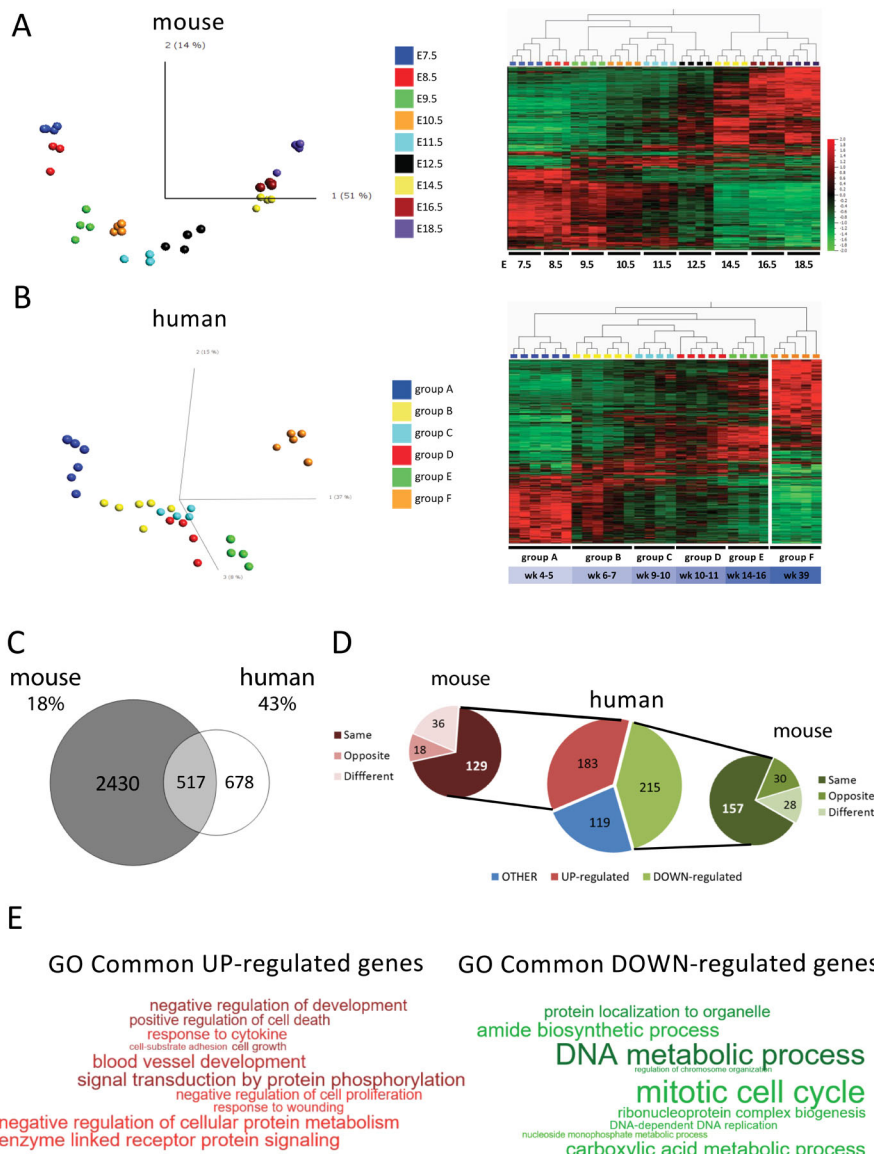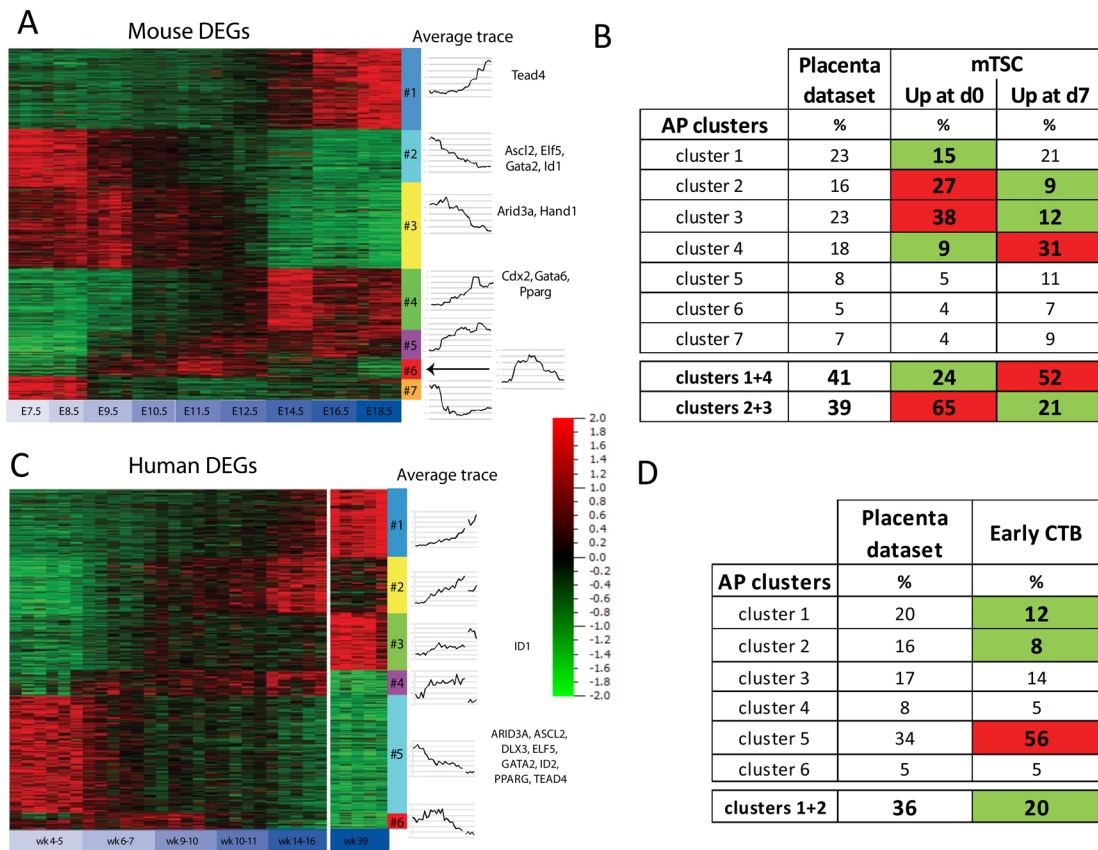
Fig. 3. Comparison of mouse and human placenta gene expression signatures across gestation. (A) Genome-wide expression profiles of mouse placentae across gestation. Samples are color-coded according to gestational age. Heatmap shows expression profiles of 2947 differentially expressed genes (DEGs, v=0.02, a multi-group analysis q<0.05, FC≥2.0). (B) Genome-wide expression profiles of human placentae across gestation. Samples are color-coded according to data-driven groups used for statistical analysis. Heatmap shows expression profiles of 1195 DEGs (v=0.02, a multi-group analysis q<0.05, FC≥2.0). (C) Venn diagram representing overlap of DEGs between mouse and human datasets. (D) Pie charts showing comparison in expression pattern direction between human and mouse common DEGs (517) (heatmaps in Fig. S3A). Central pie chart shows expression pattern in human placentae. Genes with expression pattern other than up- and downregulation across gestation were combined and labeled as 'Other'. The side charts show expression pattern comparison between the human subclasses up- and downregulated genes, and their expression patterns in mouse. (E) Biological function gene ontology (GO) terms enriched in commonly up- (red) and down- (green) regulated genes in mouse and human placentae. Font size is proportional to the enrichment −log$P$ values, with bigger font size representing higher enrichment.

differences in the precise timing of decrease in gene expression. In contrast, clusters #1, #4 and #5 showed upregulation with increasing gestational age. One cluster, #6, had a distinct pattern, with the average expression pattern showing upregulation between E9.5 and E12.5, with peak expression around E11.5, and lower expression at both extremes of gestational age. We hypothesized that genes representing trophoblast stem and/or progenitor cells would be highly represented in clusters showing an overall trend of downregulation across gestation. To this end, we differentiated mTSC for 7 days and subjected undifferentiated (day 0/d0) and day 7/d7 differentiated samples to genome-wide microarray-based RNA profiling (Arul-Nambi-Rajan et al., 2018). We then selected the DEGs between these two sample sets (v0.02, two-group analysis q0.01 and FC>2.0) and identified the AP clusters from the placental dataset in which they appeared. We found 2966 DEGs between mTSC d0 and d7 (Table S1), of which 1369 genes also appeared to be differentially expressed across gestation in the mouse placental dataset. Of the latter, 765 DEGs were upregulated in d0 TSCs; these genes were enriched (65% versus 39%) in AP clusters #2/3 (genes with high expression in early gestation placentae) and depleted (24% versus 41%) from AP clusters #1/4 (genes with high

expression in late gestation placentae) (Fig. 4B). The remaining 604 DEGs were upregulated in d7-differentiated TSCs; these DEGs were enriched (52% versus 41%) in AP clusters #1/4 (genes with high expression in late gestation placentae) and depleted (21% versus 39%) from AP clusters #2/3 (genes with high expression in early gestation placentae) (Fig. 4B). These data provide support for our hypothesis that, in fact, early gestation placentae are enriched in undifferentiated TSC-associated genes.

AP analysis on the 1195 DEGs of the human dataset yielded six clusters of co-expressed genes (Fig. 4C, Table S1). Clusters #5 and #6 both showed a trend of downregulation across gestation, though with differences in the precise pattern of decrease of gene expression. In contrast, clusters #1 through #4 generally showed upregulation with increasing gestational age, albeit with some differences, including a subsequent decrease in expression at term in clusters #2 and #4 (Fig. 4C). Clusters #2 and #4 were further distinguished based on the gestational age at which the average expression pattern began to increase: this occurred early in cluster #4 (between weeks 4-5 and weeks 6-7), and later in cluster #2 (between weeks 9-11 and weeks 14-16). We next compared these whole placental profiles with gene expression data from the CTB

A Mouse DEGs — Average trace

Clusters #1–#7. Marker genes by cluster: #1 Tead4; #2 Ascl2, Elf5, Gata2, Id1; #3 Arid3a, Hand1; #4 Cdx2, Gata6, Pparg; #6 (arrow). Timepoints: E7.5, E8.5, E9.5, E10.5, E11.5, E12.5, E14.5, E16.5, E18.5.

Color scale: 2.0, 1.8, 1.6, 1.4, 1.2, 1.0, 0.8, 0.6, 0.4, 0.2, 0.0, −0.2, −0.4, −0.6, −0.8, −1.0, −1.2, −1.4, −1.6, −1.8, −2.0

B

AP clusters	Placenta dataset	mTSC	
		Up at d0	Up at d7
	%	%	%
cluster 1	23	15	21
cluster 2	16	27	9
cluster 3	23	38	12
cluster 4	18	9	31
cluster 5	8	5	11
cluster 6	5	4	7
cluster 7	7	4	9
clusters 1+4	41	24	52
clusters 2+3	39	65	21

C Human DEGs — Average trace

Clusters #1–#6. #3 ID1; #5 ARID3A, ASCL2, DLX3, ELF5, GATA2, ID2, PPARG, TEAD4. Timepoints: wk 4-5, wk 6-7, wk 9-10, wk 10-11, wk 14-16, wk 39.

D

AP clusters	Placenta dataset	Early CTB
	%	%
cluster 1	20	12
cluster 2	16	8
cluster 3	17	14
cluster 4	8	5
cluster 5	34	56
cluster 6	5	5
clusters 1+2	36	20

Fig. 4. Affinity propagation analysis of mouse and human DEGs. (A) Affinity propagation (AP) analysis of the 2947 DEGs in the mouse dataset distinguished seven clusters of co-regulated genes. Heatmap represents expression values of genes; line graphs (right) represent the average trace for each cluster. (B) Table showing percentage distribution of mouse placental DEGs (2947 genes) across the seven AP clusters ('Placenta dataset') and of the DEGs upregulated in mTSC at day 0 ('Up at d0', 765 genes) or in day 7-differentiated mTSC ('Up at d7', 604 genes). Clusters in which genes are enriched in either mTSC d0 or d7 over the placenta dataset are highlighted in red, whereas those in which there is a relative depletion are highlighted in green. (C) AP analysis of the 1195 DEGs in the human dataset distinguished six clusters of co-regulated genes. Heatmap represents expression values of genes; line graphs (right) represent the average trace for each cluster. (D) Table showing percentage distribution of human placental DEGs (1195 genes) across the six AP clusters ('Placental dataset') and of the DEGs upregulated in the early (first trimester) CTB (week 8-10) compared with the mature CTB (week 12-39) (197 genes) (see analysis in Fig. S5A-C). Clusters in which genes are enriched in the early CTB over the placenta dataset are highlighted in red, whereas those where there is a relative depletion are highlighted in green.

isolated from different gestational age placentae (Fig. S5A,B). Unsupervised PCA and hierarchical clustering separated the CTB samples into two groups according to gestational age: those from weeks 8 and 10 (which we termed the early CTB) and those from weeks 12 and upwards, including weeks 18, 20 and 39 (which we termed the mature CTB) (Fig. S5A,B). We applied a two-group analysis on Qlucore (q0.01, FC≥2) and identified 1120 DEGs (Fig. S5C, Table S1). Of these, 197 were also differentially expressed in human placental samples throughout gestation (Fig. 4D). Interestingly, we observed an enrichment (56% versus 34%) of early CTB markers in human AP cluster #5, which showed a pattern of gene expression highest in early gestation placentae, and a relative deficit (20% versus 36%) of these markers in human AP clusters #1 and #2, which showed a pattern of gene expression highest in late gestation placentae (Fig. 4D). Again, these data suggest that, as with profiling of mouse placentae and differentiating TSC, genes enriched in early human placentae include early CTB-associated genes. Moreover, it appears that the decrease in expression of early CTB/TSC in placental samples is due not only to the decrease in the fraction of placental cells represented by these cell types, but also because the gene expression profiles of these cells are changing during gestation.

As the datasets from both species spanned the entire gestation, we wanted to see whether we could align and correlate specific gestational periods between mouse and human. To this end, we fitted non-linear curves to each of the AP clusters and computed the Euclidean distance between the curves for each mouse and each human AP cluster to identify the closest fitting human curve for each mouse curve. The 'E.d.' values shown are the sum of Euclidean distances measured across 1000 points for each pair of curves. Because of the difference in timeframe between mouse and human gestation and the large gap in our human dataset (from week 16 to term), we performed this analysis both with ['Human Long (HL)', Fig. 4C, Fig. S6A, Fig. 5A] and without the term samples ['Human Short (HS)', Fig. S5D, Fig. S6B, Fig. 5A]. Curves for mouse clusters 1, 2, 5 and 6 correlated better (smaller Euclidean distance) with the HS dataset (Fig. 5A). For clusters in which the mouse data showed closer correlation with the HL dataset (mouse clusters 3, 4 and 7), the differences between the Euclidean distances for HL and HS were generally less marked. These results show that the transcriptional patterns observed during mouse placental development more closely resemble those seen during the first half of human placental development, suggesting that human placental development possesses a long maturation phase that is not
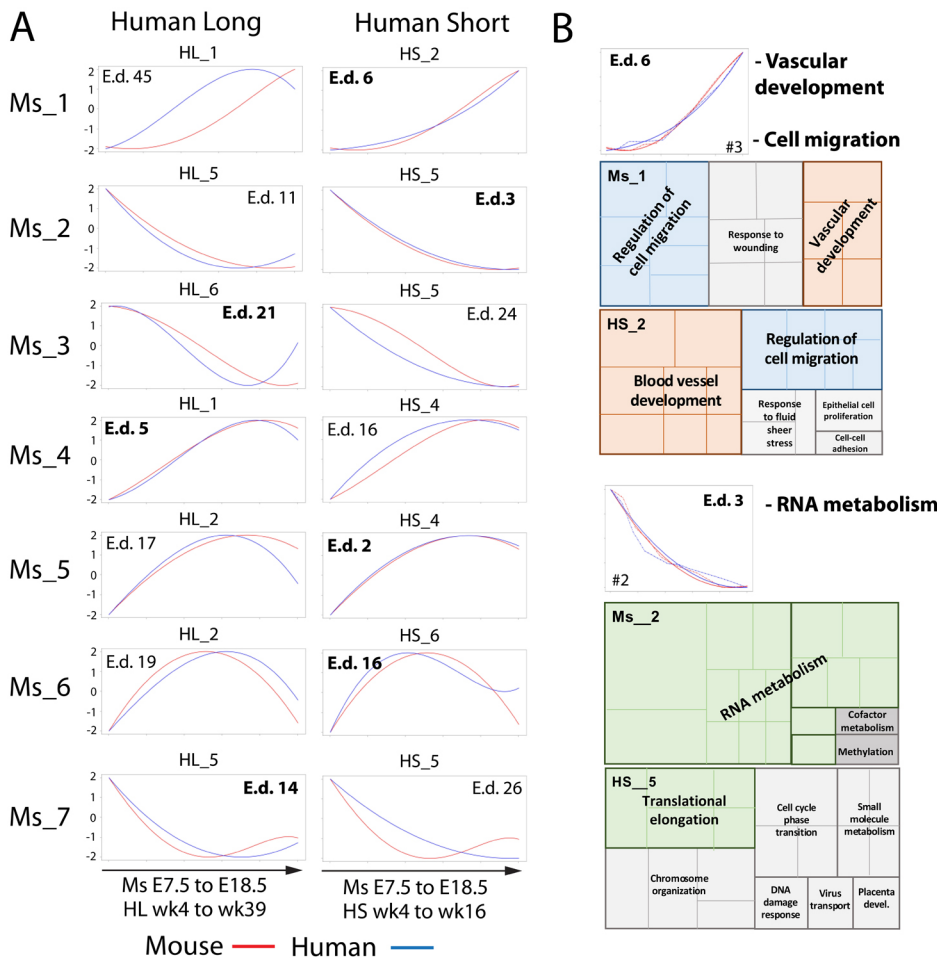
Fig. 5. Comparison of expression profiles of best-correlated mouse and human co-expression clusters. (A) Graphs showing the AP clusters from the HL dataset (which included data from term human placentae) and HS dataset (which did not include data from term human placentae) that showed the highest similarity to each mouse cluster. Data from mouse clusters are shown in red and data from human clusters are shown in blue. The Euclidean distance (E.d.) value for each pair of curves is shown. (B) Gene Ontology enrichment analysis shows overlapping function between the genes included in the cluster pairs with closely fitting curves, Ms_1/HS_2 and Ms_2/HS_5. # indicates the number of genes in common between the mouse and human clusters. Each rectangle is a representative GO term from the enrichment analysis. The representatives are joined into 'super-groups' of loosely related terms, visualized with different colors. Size of the rectangles is proportional to the P value. Overlapping functions between mouse and human clusters are marked with matching colors.

seen in the mouse. Consistent with the low percentage of overlapping genes in the mouse and human lists of DEGs, the mouse and human clusters with the closest patterns of expression across gestation did not display higher numbers of overlapping genes (Fig. S6A,B). When functional enrichment analysis of the genes in each cluster was performed (Table S2), we did observe similarities in the enriched Gene Ontology categories for two out of three pairs of clusters with the closest trajectories (Fig. 5B): mouse cluster 1 and HS cluster 2, which monotonically increase over the course of gestation, are both enriched for genes associated with vascular development and cell migration; and mouse cluster 2 and HS cluster 5, which monotonically decrease over the course of gestation, are both enriched for genes associated with RNA metabolism.

To focus our analysis on the identification of candidate genes with potential regulatory roles in early gestation, we decided to concentrate our analysis on transcription factors (TFs). Two-hundred and fifty-eight TFs were differentially expressed in the mouse dataset (Table S1) and were organized into six clusters of co-expressed genes, with the loss of cluster #7 from the AP analysis on all DEGs (Fig. S7A, compared with Fig. 4A). The expression patterns for clusters #2 and #3 were positively correlated with each other, and negatively correlated with #1, #4 and #5 (Fig. S7B). The average expression of the TFs in cluster #2 was most strongly anti-correlated with cluster #1, and cluster #3 was most strongly anti-correlated with cluster #4 (Fig. S7B). Cluster #6, which showed upregulation between E9.5 and E12.5, was not correlated or anti-

correlated with any other TF cluster. Many genes known to be involved in establishment and/or maintenance of TSC, including *Elf5*, *Gata2* and *Arid3a*, were found in clusters #2 and #3, with downregulation of expression with increasing gestational age (Fig. S7A). Surprisingly, however, two TSC-associated genes, *Tead4* (cluster #1) and *Cdx2* (cluster #4), displayed the opposite expression pattern, increasing with gestational age. To validate these latter findings, we performed *in situ* hybridization on mouse placenta samples across gestation, using probes specific to *Tead4* (Fig. 6A) or *Cdx2* (Fig. 6B). We noted that, consistent with the microarray results, the expression of these transcripts, as determined by *in situ* hybridization is significantly elevated later in gestation, with *Tead4* expressed through all layers of the mouse placenta (Fig. 6A) and *Cdx2* expressed specifically in the junctional zone in later gestation placentae, particularly in PAS-positive glycogen cells (Fig. 6B).

In the human dataset, 115 TFs were differentially expressed (Fig. S7C, Table S1) and were organized into five clusters of co-expressed genes, with the loss of cluster #6 from the AP analysis on all DEGs (Fig. S7C, compare with Fig. 4C). Human TF cluster #4, similar to the mouse cluster #6, included TFs with highest expression around mid-gestation. Human TF clusters #1, #2 and #3 were anti-correlated to TF cluster #5 (Fig. S7D), which is enriched in genes upregulated in early CTB and includes many known progenitor markers. As mouse TF clusters #2 and #3 and human TF cluster #5 were all enriched in trophoblast stem and/or progenitor markers, we compared the gene lists in these clusters. In both species, these clusters included well-known progenitor
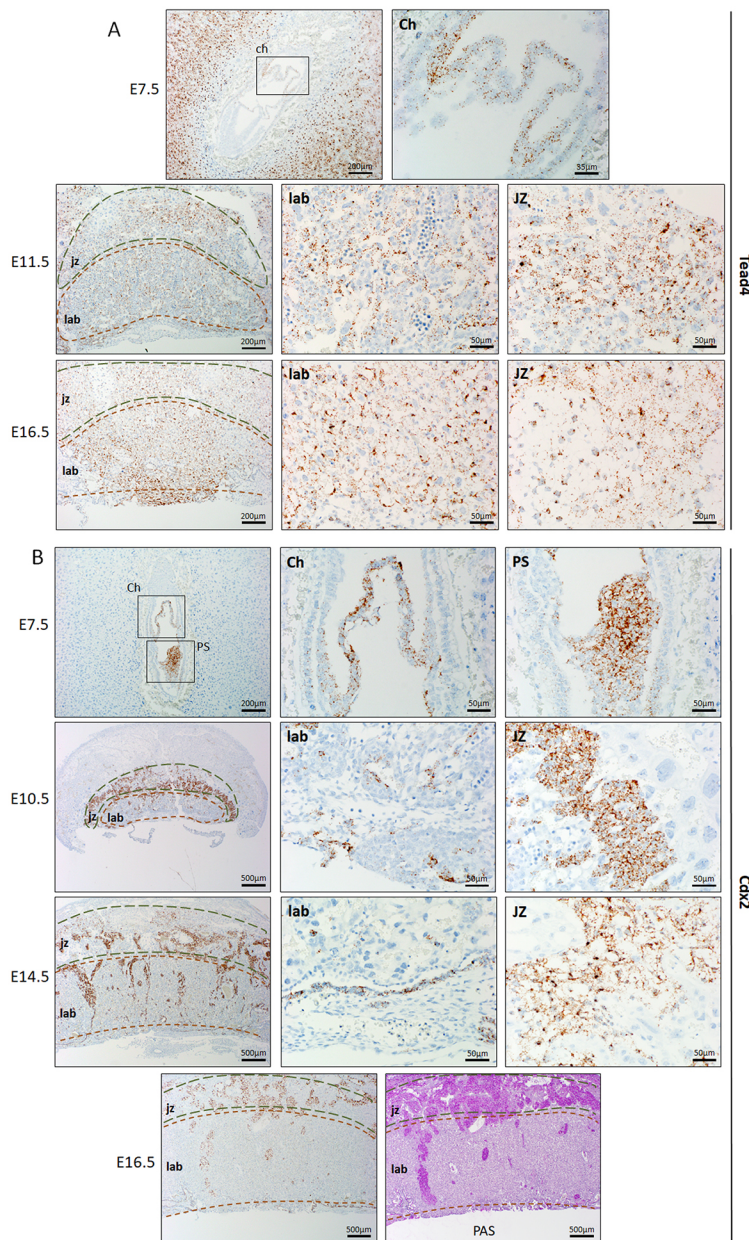
Fig. 6. *In situ* hybridization for Cdx2 and Tead4 in mouse placentae confirms upregulation with increasing gestational age. (A) *In situ* hybridization for Tead4. Tead4 expression was observed in the chorion (ch) at E7.5, and in both the labyrinth (lab) and the junctional zone (jz) at E11.5 and E16.5. (B) *In situ* hybridization for Cdx2. Cdx2 expression was observed in the chorion (ch) and primitive streak (PS) at E7.5, and in the labyrinth (near the chorionic plate, lab) and junctional zone (jz) later in gestation. PAS staining in a consecutive section at E16.5 indicates Cdx2 expression in glycogen cells.

markers, such as Elf5/ELF5, Arid3a/ARID3A and Gata2/GATA2. However, there were also large numbers of species-specific TFs, which might account for the differences between mouse and human placental development. In particular, we noticed the presence of VGLL1, a homolog of the *Drosophila* Vestigial factor, in human cluster #5, but not in any mouse cluster. Recent studies have suggested an interaction between VGLL1 and TEAD4 (also present in human cluster #5, Fig. S7D), creating a protein complex potentially able to promote the transcription of specific downstream targets (Pobbati et al., 2012). Given the role of TEAD4 in trophoblast lineage specification in the mouse (Nishioka et al., 2008; Yagi et al., 2007), we considered that VGLL1 may be an interesting regulatory gene candidate as a human-specific early CTB marker. Knowledge regarding the function of VGLL1 during development is extremely limited; therefore, we decided to begin by evaluating the localization and expression patterns of VGLL1/Vgll1 in the placentae of both species across gestation.

VGLL1 is a human-specific CTB marker
In human placentae, immunohistochemistry revealed high expression of VGLL1 in villous CTB and proximal cell column (pCC) trophoblast in early first trimester samples (week 6, Fig. 7A); there was overlap with TEAD4 expression in villous CTB, but not in pCC trophoblast (Fig. 7A). Moreover, cells expressing VGLL1 co-expressed PCNA, a marker of cell proliferation (Fig. S8A). The expression of both VGLL1 and TEAD4 was maintained in the CTB across gestation (Fig. 7B,C); but unlike TEAD4, VGLL1 was also expressed in mature EVT at the basal plate of term placentae (Fig. 7C). To confirm the specificity of VGLL1 antibody, we performed *in situ* hybridization using VGLL1-specific probes, and identified mRNA expression in the same cells in the early human placenta (Fig. S8B). In contrast, in mouse placentae, we could not detect any Vgll1 mRNA by *in situ* hybridization at any gestational age (Fig. S9A and data not shown). Human VGLL1 expression in CTB was further confirmed by western blot, with the isolated primary
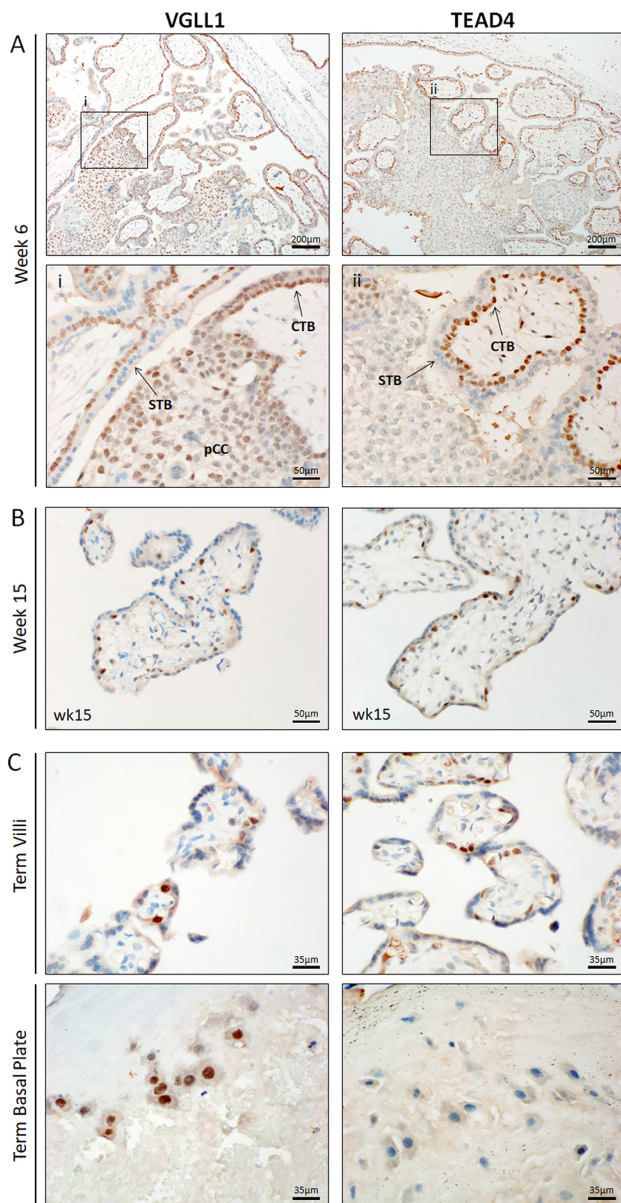
Fig. 7. VGLL1 and TEAD4 are co-expressed in the human villous cytotrophoblast across gestation. (A) In early post-implantation human placenta, VGLL1 and TEAD4 are co-expressed in the villous cytotrophoblast (CTB). Extravillous trophoblast in the proximal cell column (pCC) expresses VGLL1 but not TEAD4. (B) In second trimester placentae, the villous CTB (now discontinuous) maintains expression of both VGLL1 and TEAD4. (C) At full term, VGLL1 expression is visible both in the persistent villous CTB (term villi) and also in the mature extravillous trophoblast (term basal plate). TEAD4 expression is restricted to the villous CTB. CTB, cytotrophoblast; pCC, proximal cell column; STB, syncytiotrophoblast; wk, week.

CTB showing high levels of VGLL1 protein, with decreasing expression upon differentiation of these cells *in vitro* (Fig. 8A). In contrast, no Vgll1 protein was expressed in either undifferentiated or differentiated mTSC (Fig. S9B), suggesting a species-specific role for VGLL1 in human, but not mouse, trophoblast.

To further probe the role of VGLL1 in the human early CTB, we used a previously established BMP4-based two-step protocol for differentiation of human embryonic stem cells (hESCs) into CTB-like cells (step 1), and then into mature terminally differentiated EVT- and STB-like cells (step 2) (Horii et al., 2016). We evaluated

VGLL1 mRNA expression and found it to be upregulated during the first step of this protocol, along with downregulation of *POU5F1/OCT4* expression and upregulation of other known human early CTB markers, *TP63* and *CDX2* (Fig. 8B); *TEAD4* expression did not change significantly, as previously shown in similar BMP4-treated hESCs (Home et al., 2012) (Fig. 8B). VGLL1 protein expression was confirmed in these hESC-derived CTB-like cells by western blot (Fig. 8C). Immunofluorescence staining confirmed lack of VGLL1 in undifferentiated OCT4^{+} hESC and positive expression in nuclei of KRT7^{+} hESC-derived CTB-like cells at day 4 (Fig. 8D and Fig. S10A-C). hESC-derived CTB-like cells also showed nuclear expression of TEAD4, as previously reported (Home et al., 2012), colocalizing with VGLL1 (Fig. S10C). We also generated hESC lines, using a mix of five shRNA constructs targeting VGLL1, and noted that VGLL1 knockdown resulted in blunted expression of the CTB marker TP63 in hESC-derived CTB, without affecting downregulation of POU5F1/OCT4 (Fig. 8E).

DISCUSSION

Owing to both practical and ethical issues, early placental development is often studied in non-human animal models; in particular, the mouse. However, an increasing body of evidence has identified significant species-specific differences in early embryonic development, including in specification and differentiation of the trophectoderm (TE), between mouse and human. Here, we have performed a comprehensive comparative study of mouse and human placental development, with a particular focus on defining expression of known mouse trophoblast stem and/or progenitor markers in the human placenta, and identification of novel human-specific early CTB markers. We began our study by evaluating expression and localization of three key markers of mouse TSC: Cdx2, which is required for TE specification (Strumpf et al., 2005), and Eomes and Elf5, which reinforce and maintain the TSC state (Donnison et al., 2005; Ng et al., 2008; Russ et al., 2000). Consistent with a prior study reporting co-expression of CDX2 and ELF5 proteins in the CTB of early gestation human placenta (Hemberger et al., 2010), we also noted that CDX2 was particularly abundant in the CTB of early gestation placentae, with a higher percentage of CDX2^{+} CTB cells close to the chorionic plate (fetal surface). However, we were not able to detect specific nuclear staining with multiple commercially available antibodies against ELF5, including the one used in a previous publication (Hemberger et al., 2010) (data not shown). Using *in situ* hybridization, we found that *ELF5* mRNA was expressed in both villous CTB and trophoblast cells of the proximal column, both of which are proliferative trophoblast (Lee et al., 2007).

Unlike CDX2 and ELF5, however, EOMES expression was conspicuously absent from all human placenta samples tested. EOMES expression has been documented by immunostaining in early human blastocysts (Zdravkovic et al., 2015) and putative trophoblast stem cells (Genbacev et al., 2011); however, cytoplasmic staining patterns noted in these cells raise issues regarding the specificity of these antibodies. Our data are consistent with a recent study evaluating gene expression in the pre-implantation human embryo by single-cell RNA-seq, showing a lack of EOMES expression in human TE (Blakeley et al., 2015). Based on co-expression of ELF5 and CDX2 in a subset of CTB, we concur with Hemberger and colleagues (Hemberger et al., 2010) that it is highly likely that early post-implantation human placenta harbors TSCs. The lack of EOMES expression, however, indicates that establishment and maintenance of TSCs in the human placenta requires other factors.
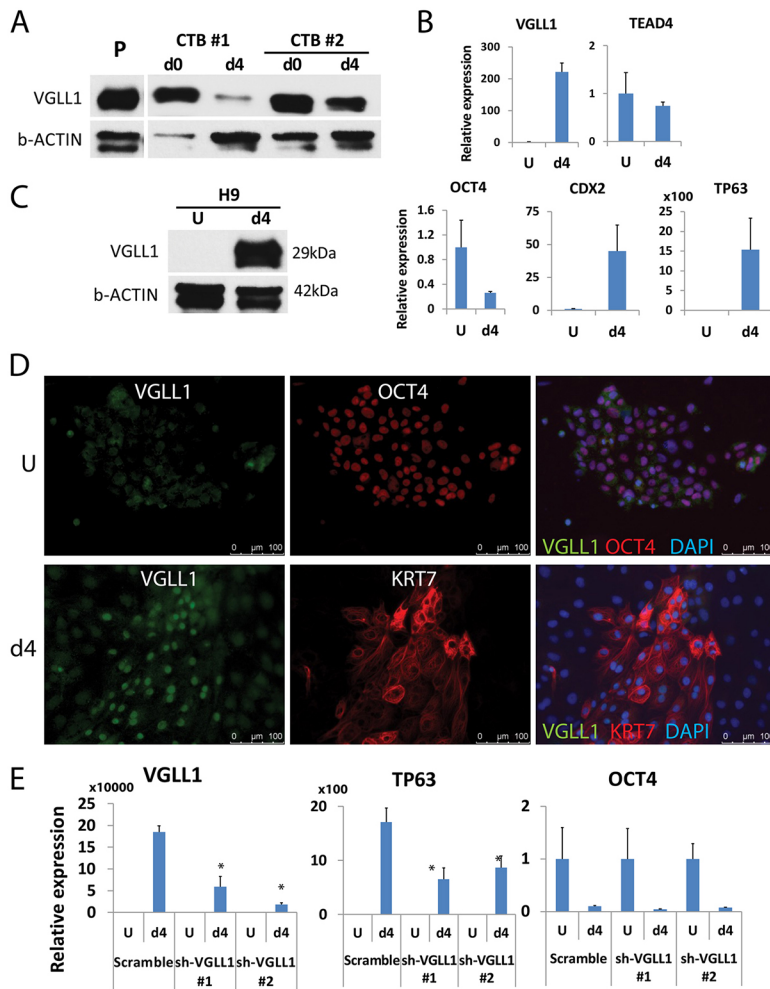
Fig. 8. VGLL1 is expressed in primary and hESC-derived CTB *in vitro*. (A) Western blot analysis of VGLL1 and β-actin (loading control) in week 6 whole placenta (P) and primary first trimester CTB (#1, week 13; #2, week 11). Expression was analyzed both in freshly isolated CTB (d0) and in differentiated CTB (d4). (B) qRT-PCR analysis of VGLL1, TEAD4, CTB markers (TP63 and CDX2) and a pluripotency marker (OCT4) in undifferentiated hESCs (U) and in hESC-derived CTB-like cells (d4) following step 1 of our two-step BMP4-based trophoblast differentiation protocol (Horii et al., 2016) (*n*=3). (C) Western blot analysis of VGLL1 and β-actin (loading control) in undifferentiated H9 hESCs (U) and in hESC-derived CTB-like cells (d4). (D) Double immunostaining of undifferentiated H9 hESC (U) and hESC-derived CTB-like cells (d4) with VGLL1 and either OCT4 (top) or pan-trophoblast marker KRT7 (bottom). (E) qRT-PCR analysis of VGLL1, TP63 and OCT4 in hESC clones stably expressing either scrambled or VGLL1-targeting shRNA. *n*=3, *$P<0.05$ compared with scramble d4.

Examining individual markers in this fashion is time-consuming and labor intensive. We therefore decided to compare mouse and human placental gene expression across gestation using more comprehensive microarray-based gene expression technology. For both species, we started collection at the earliest post-implantation timepoint we could confidently sample: gestational week 4 for human and E7.5 for mouse. Although our mouse data spanned most of the post-implantation gestational period in a uniform manner, our human data were bimodally distributed, with dense coverage of the first trimester and the late third trimester. The reasons for this species-specific difference are twofold: one is related to our overall questions, as we were interested in characterizing the human CTB in early gestation; the second is due to practical reasons, as acquisition of 'normal' tissues from late second and early third trimesters is difficult at best.

One challenge encountered in cross-species comparative studies is from integration of species-specific datasets. Although we paid particular attention to selecting results from the most-robust and representative probe, when multiple probes for a given transcript were available, this selection process might have introduced bias into the analysis. Moreover, discrepancy between mouse and human gene orthologs further complicated the analysis. However, the design of our analysis, in which we first identified DEGs within each species across gestational age, allowed us to avoid many of the potential artifacts that might arise from the use of different probes for the mouse and human transcripts. The large dataset gathered in this study represents an invaluable resource for both mouse and

human placentologists and developmental biologists to evaluate gene expression in this important transient organ throughout gestation and probe the role of specific genes and pathways during its development. In our overall inter-species comparison of gestational periods, we noted a closer fit between the patterns observed in the mouse and human placentae when the comparison was restricted to mouse placentae from E7.5-18.5 and to human placentae from weeks 4-16, rather than including human term placentae, suggesting that the developmental timeline in mouse runs parallel to the first half of human development. In addition, our data support the concept that, although general biological processes and regulatory programs associated with different stages of placental development partially overlap between mouse and human, there are distinct species-specific regulatory interactions underlying this process. This is supported by limited overlap between the two species at the individual transcript level, both in the sets of differentially expressed transcripts in early compared with late gestation, and in clusters of co-expressed genes that show similar patterns of expression across gestation in both species. In some cases (e.g. Tead4/TEAD4), the same factor may display different gestational age-specific expression patterns in mouse and human placentae, whereas in other cases (e.g. Eomes in mouse and VGLL1 in human), a factor appears to play a role in one species but not the other. Interestingly, our data from human placentae showed significant changes in gene expression even within the first trimester, reflecting rapid development of the placenta in this timeframe. The most rapid changes occurred from week 4 to week 8,

with subsequent slowing of the rate of change. In comparison, the mouse placenta showed changes throughout the entire gestation period and lacked the long maturational plateau present in human placental development. Although we cannot completely rule out that this observation might be biased due to sparser human samples at later gestational ages, for reasons described above, it is consistent with rapid changes in placental morphology and size during the first trimester. We thus suggest that future studies using first trimester human placental samples specify the week of gestation.

For this study, we focused our analysis on genes that display a progressive decrease in expression according to gestational age in human and mouse placentae. As trophoblast progenitor cells (CTB in the human placenta and TSC in the mouse) are known to be more abundant in early gestation placentae (Lee et al., 2007; Natale et al., 2017), at least some of the genes enriched in early gestation placentae would thus likely correspond to these cell populations. To identify genes that potentially maintain such cell populations, we further focused our attention on transcription factors (TFs), which are known to orchestrate important cellular functions by regulating gene expression. Although some TFs known to be involved in early mouse TSC specification/maintenance were enriched within early gestation placental tissues (including Elf5, Gata2, Arid3a), two TFs, Cdx2 and Tead4, showed a surprisingly different pattern, with increased expression in later gestation placentae; we confirmed these data by *in situ* hybridization. Although Tead4 is known to be involved in trophoblast lineage specification in the pre-implantation mouse embryo (Nishioka et al., 2008; Yagi et al., 2007), studies from Jacquemin and colleagues have reported expression of Tead4 in the labyrinth (Jacquemin et al., 1996, 1998). With the sensitive *in situ* hybridization technique used in this study, we observed localization in both the labyrinth and junctional zone of the mouse placenta. Similarly, Cdx2 was found to be expressed not just in extra-embryonic ectoderm and primitive streak in the early embryo, as previously shown (Beck et al., 1995; Strumpf et al., 2005), but also in the junctional zone of the later gestation mouse placenta. Reports of this expression date back to Beck and colleagues in 1995, but we were able to confirm localization of Cdx2 to PAS-positive glycogen cells. Further studies are required to determine the role of both of these TFs in the late gestation mouse placenta.

Similar analysis of human placenta across gestation identified ELF5, TEAD4, GATA2 and ARID3A as being enriched in early gestation tissues, although neither EOMES nor CDX2 was identified in any specific clusters due to very low/undetectable mRNA levels. Although the former correlates with our *in situ* hybridization data, the latter is likely due to random sampling of placental tissues, without regard to proximity to the chorionic plate. This highlights one of the limitations of this study, at least with the human placenta, as we investigated gene expression in a random sampling of villous tissue, containing a mixed cell population, with stromal tissues as well as trophoblasts. Single-cell transcriptome analysis might overcome this limitation in the future, although common issues associated with these techniques, such as sampling and sample size, will need to be addressed. Yet another known early human CTB factor not identified as a DEG in our dataset was GATA3 (Deglincerti et al., 2016; Lee et al., 2016). In fact, in complex with the AP-2 transcription factors TFAP2A and TFAPC, GATA3 was recently identified as an early repressor of pluripotency/inducer of trophectoderm during BMP4-induced trophoblast differentiation of human embryonic stem cells (Krendl et al., 2017). We performed *in situ* hybridization on human placenta samples across gestation with a GATA3-specific probes and found expression of this marker in all trophoblast subtypes, including

syncytiotrophoblast and extravillous trophoblast (data not shown); this is consistent with previous immunolocalization studies of this protein in gestational tissues (Banet et al., 2015). This finding highlights yet another limitation of our study, where factors that are not unique to CTB, yet serve an important function in these cells, may have escaped identification.

In the TF cluster enriched in early gestation human placentae, among putative trophoblast progenitor markers, including ELF5, ARID3A (Rhee et al., 2017) and TEAD4, we identified VGLL1, a homolog of *Drosophila* vestigial gene, as being uniquely expressed in human (and not the mouse) placenta. Very little is known about VGLL1 function; however, it is known to bind TEAD proteins through its vestigial homology domain (Vaudin et al., 1999). Interestingly, structural analysis of the complex has shown that VGLL1 binds to the same pocket in TEAD4 to which YAP/TAZ proteins bind (Pobbati et al., 2012). As the combination of Tead4 and Yap occurs in mouse TE, leading to induction of Cdx2 (Home et al., 2012; Nishioka et al., 2009), we hypothesized that VGLL1 may be involved in similar events, but specific to the human placenta. We showed that VGLL1 protein was specifically expressed in CTB and proximal cell column trophoblast, where proliferative trophoblast reside in the early human placenta. However, VGLL1 colocalized with TEAD4 only in CTB. Moreover, we observed VGLL1 to be upregulated during trophoblast differentiation of human embryonic stem cells, induced by BMP4; Krendl et al. (2017) have recently confirmed this finding, identifying VGLL1 to be induced, following induction of GATA factors, after BMP4 treatment of these cells. Interestingly, in *Xenopus*, Vgll1 was found to be expressed in the epidermis, and noted to be induced downstream of BMP4 (Faucheux et al., 2010). Downregulation of VGLL1 in hESC resulted in blunted expression of the human CTB-associated marker TP63 following BMP4 treatment. We have previously shown that TP63, a CTB marker unique to the human placenta, is required for BMP4-induced trophoblast differentiation of hESC (Li et al., 2013). Our new data now indicate that VGLL1 may be a human-specific regulator of trophoblast differentiation, possibly acting in concert with TEAD4, to regulate TP63 expression.

Overall, this study represents the first attempt at a large-scale comparison between mouse and human placental development from early post-implantation period to term. Our data have identified species-specific genes and networks of TFs involved in placental development. Specifically, we have begun to characterize VGLL1 as a marker specific to human trophoblast and we posit a potential role for the TEAD4/VGLL1 complex during early human trophoblast differentiation. Further studies will be necessary to investigate the specific role of this complex, and its upstream regulation and downstream effectors, in human placental development.

MATERIALS AND METHODS
Placental samples

weeks 7 and 10; and three for week 6), seven second trimester (one per weeks 13, 14, 15, 17, 18, and two for week 20) and three full-term samples. Gestational age was determined based on crown-rump length, as measured on first trimester ultrasound, and was stated in weeks from the first day of the last menstrual period; in the text, it is listed according to the completed week of gestation (i.e. placentae at week 4 day 0, through week 4 day 6 were defined as 'week 4'). For placentae from pre-viable gestations, 'normal' is defined as a singleton pregnancy without any detectable fetal abnormalities on ultrasound; for full-term placentae, 'normal' is defined by a non-hypertensive, non-diabetic singleton pregnancy, where the placenta is normally grown and shows no gross or histological abnormalities.

Mouse placental samples were collected according to a UCSD IACUC-approved protocol. CD-1 mice were time-mated and the presence of the morning plug represented E0.5 of gestation. Fifty-four placenta samples were used for the microarray analysis: five biological replicates from two different litters were collected at E7.5, 8.5, 9.5, 10.5, 11.5, 12.5, 14.5, 16.8 and 18.5. Two placentas per time point were stained.

Primary cytotrophoblast (CTB) isolation

When not specified, media components in the methods section were purchased from Gibco-Life-Technology. Human CTB cells were isolated from first trimester placentae according to the protocol described by Wakeland et al. (2017). Briefly, chorionic villi were minced and subjected to three sequential digestions. Collected cells were separated on a Percoll (Sigma-Aldrich) gradient. About 2 million freshly isolated cells were lysed for western blot and about 2 million cells were plated on fibronectin (20 µg/ml; Sigma-Aldrich) and cultured in Dulbecco's modified Eagle's medium/F12 containing 10% fetal bovine serum (Sigma-Aldrich), penicillin-streptomycin (Thermo Fisher), and gentamicin for 4 days in 2% oxygen before lysis. Human cytotrophoblast cells were isolated from second trimester and term placentae, based on the protocol described by Li et al. (2013). CTB from gestational weeks 8, 10, 12 and 18 (two each), one 20 week and two full-term placentae were isolated and subjected to microarray-based gene expression profiling as described below.

Stem cell culture

Use of human embryonic stem cells was approved by the UCSD Embryonic Stem Cell Research Oversight Committee. H9/WA09 human embryonic stem cells (hESCs) were cultured in Stem-Pro media containing 12 ng/ml bFGF (BioPioneer) on geltrex-coated plates and passaged as necessary with StemDS (ScienCell). Trophoblast differentiation was induced according to the 2-step protocol developed in the lab (Horii et al., 2016) and samples collected at the CTB-like stage. Briefly, 60,000 H9 hESCs were seeded onto geltrex-coated six-well plates in EMIM minimal media (knock-out DMEM/K12 media containing 2 mM L-glutamine, 1 mg/ml ITS, 2% BSA, 100 ng/ml heparin and MEM non-essential amino acids). After 48 h, 10 ng/ml BMP4 (R&D Systems) was added to the EMIM media and cells were cultured for 4 days. Media were changed every day.

Five Mission shRNA Lentiviral constructs targeting the human VGLL1 gene were purchased and packaged into lentiviral particles according to the manufacturer's instructions (Sigma-Aldrich). Lentiviral supernatants containing a mix of all five VGLL1-targeting constructs or a scramble control sequence were concentrated with PEG-it virus-precipitation solution (System Biosciences). H9 hESCs were infected with the concentrated viral particles and 8 µg/ml polybrene (Sigma). Stable clones were selected with 10 µg/ml of puromycin. Packaging and infection efficiency were tested using a GFP-expressing lentivirus. Two independently derived clones, which showed the best knock-down, were used in further experiments.

Mouse trophoblast stem cells derived in the lab were cultured in feeder-free condition in differentiation media containing RPMI 1640 media (Corning, Manassas, USA), 20% fetal bovine serum (Sigma-Aldrich), 1 mM sodium pyruvate (Invitrogen), 2 mM L-glutamine, 55 nM 2-mercaptoethanol (Invitrogen) and the addition of the growth factors FGF4 (25 ng/ml, Sigma-Aldrich), activin A (10 ng/ml, Stemgent) and heparin (1 µg/ml, Sigma) to keep them undifferentiated. Cells were differentiated as previously described by Moretto Zita et al. (2015).

Immunohistochemistry and in-situ hybridization

Placental tissue samples were fixed in neutral-buffered formalin and embedded in paraffin wax. Sections (5 µm) were subjected to either immunohistochemistry or in situ hybridization, both performed on a Ventana Discovery Ultra automated stainer (Ventana Medical Systems). For immunohistochemistry, standard antigen retrieval was performed for 24-40 min at 95°C as per the manufacturer's protocol (Ventana Medical Systems). The following primary antibodies were incubated for 1 h at 37°C: rabbit anti-CDX2 (EPR2764Y, 1:100; Abcam), rabbit anti-VGLL1 (HPA042403, 1:100; Sigma-Aldrich) and rabbit anti-TEAD4 (HPA056896, 1:20; Sigma-Aldrich). Staining was visualized using 3,3′-diaminobenzidine (DAB, Ventana Medical Systems) and slides were counterstained with Hematoxylin. For in situ hybridization, slides were de-paraffinized, and subjected to antigen retrieval and protease treatment as described by the manufacturer (ACD-Bio). In situ hybridization was performed using the RNAscope method with probes specific to human ELF5, EOMES, GATA3 and VGLL1, and to mouse Cdx2, Tead4 and Vgll1, as well as a negative control probe (DapB), all from ACD-Bio. Following amplification steps, the probes were visualized using DAB and slides counterstained with Hematoxylin. Both immunohistochemistry and in situ hybridization slides were analyzed by conventional light microscopy on an Olympus BX43 microscope (Olympus). For in situ hybridization, each dot corresponds to a single RNA message transcript; larger dots may be multiple mRNAs closely localized. Probes and antibodies were tested on known positive control tissues prior to use on the above placental tissues.

Immunofluorescence

hESCs were cultured on geltrex-coated coverslips and fixed with 4% PFA/PBS (VWR International) for 15 min. Cells were incubated in 0.1% Triton X-100 (Bio-Rad Lab) for 15 min and in blocking buffer (0.1% Triton X-100, 5% goat serum and 1% BSA in PBS) for 1 h both at room temperature before overnight staining in primary antibodies at 4°C. The following primary antibodies, diluted in blocking buffer, were used: anti-KRT7 (mouse, Invitrogen Clone OV-TL 12/30, 1:100; or rabbit, Abcam ab68459, 1:100), anti-OCT4 (rabbit polyclonal, Abcam #ab19857, 1:200; or mouse monoclonal, Santa Cruz sc-5279, 1:100), anti-TEAD4 (mouse monoclonal, Abcam ab58310, 1:100) and anti-VGLL1 (rabbit, Sigma-Aldrich, HPA042403, 1:100). Immunofluorescence on a paraffin-embedded placenta (week 9) was performed after antigen retrieval according to the manufacturer's guidelines. Tissue was incubated overnight with anti-VGLL1 (rabbit, Sigma-Aldrich, 1:500) and anti-PCNA (mouse, Abcam ab29, 1:500). After PBS washes, cells and tissues were incubated with AlexaFluor-488 or -594-conjugated goat anti-rabbit or anti-mouse secondary antibodies (1:500, Thermo Fisher) for 2 h at room temperature. Nuclei were stained with DAPI during final washing steps. Coverslips were mounted on glass slides with Hard-set Vectorshield mounting media (Thermo Fisher) and visualized under a Leica STP 6000 fluorescent microscope.

Western blot

Cells were lysed in protein lysis buffer (1% Triton X-100 and 0.5% SDS in TBS) containing HALT protease inhibitor cocktail (Thermo Fisher) and 5 mM EDTA and sonicated. Protein lysates were quantified using a Pierce BCA assay (Thermo Fisher). Thirty micrograms of protein were loaded onto 12.5% or 14% SDS gels and separated by gel electrophoresis followed by transfer onto PVDF membrane. Membranes were probed with 1 µg/ml of anti-human VGLL1 (rabbit, Sigma, HPA042403), anti-mouse VGLL1 C-terminal (rabbit, Abcam, ab171019) or anti-β-ACTIN (mouse, Sigma-Aldrich #A5441) antibodies overnight at 4°C followed by HRP-conjugated anti-rabbit and anti-mouse antibody (1:2000, Cell Signaling Technology) incubation for 1 h at room temperature. Luminol reaction was performed using Pierce ECL Western Blotting Substrate (Thermo Fisher) and exposed film was processed in an automatic medical film processor machine SRK-101A (Konica Minolta).

RNA purification, total RNA microarray-based gene expression profiling and q-RT-PCR

Total RNA was purified using the MirVana RNA extraction kit (Ambion). For microarray analysis, total RNA was quantified using the Ribogreen

reagent (Life Technology) and quality controlled on a Bioanalyzer (Agilent). Samples with RIN>8.0 were selected for microarray analysis. Two-hundred nanograms of total RNA were amplified and labeled using the TotalPrep kit (Ambion). The labeled product was then hybridized and scanned on a BeadArray Reader (Illumina) according to the manufacturer's instructions. Illumina HT12 was used for human placental tissues; MouseRef-8 v2.0 for mouse samples. Data have been uploaded into the Gene Expression Omnibus (GEO) database (Edgar, 2002) under GSE100053 and GSE100279 (Arul-Nambi-Rajan et al., 2018). For qPCR, total RNA was quantified with a Nanodrop and 500 ng were reverse transcribed with iScript RT kit (Bio-Rad). Four microliters of diluted cDNA were used in each qPCR reaction with Power SYBR green PCR Mastermix (Applied Biosystems) and 1.25 µM of target primers. Data were analyzed according to the ddCt method using 18S as housekeeping gene. Statistical analysis was performed on the normalized Ct values (dCt) using either the unpaired t-test or ANOVA with Tukey's post-hoc test. Primer sequences are shown in Table S3.

Microarray data analysis

Only genes represented in both species were analyzed and one single probe per gene was selected when multiple probes were available (the probe with the lowest average detection P value and highest mean AVG signal was selected). Genes were filtered for an average detection $P<0.01$ and normalized in R using Robust Spline Normalization in the lumi package. Using the PCA and heatmap functions in Qlucore Omics Explorer 3.1, outliers were removed and samples were grouped according to gestational age in a data-driven manner, as described in the Results section. Differentially expressed genes (DEGs) were identified applying a variance cutoff of 0.02, a multi-group comparison statistical analysis (similar to ANOVA) with q<0.05, and a fold change of at least 2.0 in at least one of the group pairs. The same analysis was applied to the GEO dataset GSE11224 by Knox and Baker (2008) and the list of DEGs compared with our dataset. Gene Ontology enrichment analysis for Biological Process was performed using Metascape (http://metascape.org) (Tripathi et al., 2015). Affinity propagation (AP) algorithm (Dueck and Frey, 2007) under an R implementation (Bodenhofer et al., 2011) was used to cluster differentially expressed genes or transcription factors (TFs), using Pearson correlations as the similarity measure. Genes were designated to be transcription factors if the Gene Ontology terms assigned to them included the word 'transcription'. The most highly connected TFs were identified by calculating the sum of all positive and negative Pearson correlations of each TF with the others, called sum score positive and sum score negative, respectively. TFs with absolute positive and negative sum score values of at least 40 for mouse and at least 20 for human were retained. For these filtered TF lists, we then applied absolute Pearson correlation thresholds of at least 0.75 for mouse and at least 0.6 for human (i.e. keeping only highly correlated connections); subsequently TFs with fewer than three highly correlated connections were removed. AP results for transcription factors were visualized in Cytoscape (Shannon et al., 2003), in which the nodes represented TFs and the edges represented the Pearson correlation between TFs. For the mouse data, which contained markedly more TFs, node size was set to a fixed value to enable visualization of each node, whereas, in the human dataset, node size represented the positive or negative sum score (as indicated). Node colors indicate the assigned AP cluster. The edge thickness reflected the Pearson correlation values, where blue indicated positive and red indicated negative correlation. We used the Prefuse Force Directed layout in Cytoscape with Pearson correlation set as the attribute that contains the weights. The default parameter values were used, except that the Spring Length was set to 150. In order to compare the gene expression pattern across gestation revealed by the AP analysis between mouse and human, we average the expression values for each cluster at each time point.

Microarray dataset comparison between species

Cytoscape (Shannon et al., 2003) was used to visualize the species-specific GO enrichment analysis and to connect terms with overlapping functions. To fit a curve to the pattern of expression across gestation for each AP cluster, we calculated the average expression level for all genes in each cluster, scaled the average values for each cluster across samples (mean=0,

variance=2) and then identified the optimal function f(x), where x is the gestational age. To identify the best functions, we tested several methods, including linear regression (e.g. Gaussian processes, kernel quartile, principal components, partial least squares and least squares) and nonlinear regression (e.g. support vector with polynomial kernel and genetic algorithms, in which the elementary functions used are power and exponential functions). For all methods, the objective function used was the error function. For all clusters, the functions obtained using genetic algorithms were always the best fit with the experimental data (i.e. had the smallest errors, Table S4). Therefore, the curves included in the manuscript are those derived from the genetic algorithm approach. Gene Ontology enrichment analysis for Biological Process was performed using Metascape (http://metascape.org) (Tripathi et al., 2015) and visualized on REVIGO using TreeView (Supek et al., 2011).

References

Arul-Nambi-Rajan, K., Khater, M., Soncin, F., Pizzo, D., Moretto-Zita, M., Pham, J., Stus, O., Iyer, P., Tache, V., Laurent, L. C. et al. (2018). Sirtuin1 is required for proper trophoblast differentiation and placental development in mice. *Placenta* **62**, 1-8.

Banet, N., Gown, A. M., Shih, I.-M., Li, Q. K., Roden, R. B. S., Nucci, M. R., Cheng, L., Przybycin, C. G., Nasseri-Nik, N., Wu, L.-S.-F. et al. (2015). GATA-3 expression in trophoblastic tissues: an immunohistochemical study of 445 cases, including diagnostic utility. *Am. J. Surg. Pathol.* **39**, 101-108.

Beck, F., Erler, T., Russell, A. and James, R. (1995). Expression of Cdx-2 in the mouse embryo and placenta: possible role in patterning of the extra-embryonic membranes. *Dev. Dyn.* **204**, 219-227.

Blakeley, P., Fogarty, N. M. E., del Valle, I., Wamaitha, S. E., Hu, T. X., Elder, K., Snell, P., Christie, L., Robson, P. and Niakan, K. K. (2015). Defining the three cell lineages of the human blastocyst by single-cell RNA-seq. *Development* **142**, 3613-3613.

Bodenhofer, U., Kothmeier, A. and Hochreiter, S. (2011). Apcluster: an R package for affinity propagation clustering. *Bioinformatics* **27**, 2463-2464.

Cuffe, J. S. M., Holland, O., Salomon, C., Rice, G. E. and Perkins, A. V. (2017). Review: placental derived biomarkers of pregnancy disorders. *Placenta* **54**, 104-110.

Deglincerti, A., Croft, G. F., Pietila, L. N., Zernicka-Goetz, M., Siggia, E. D. and Brivanlou, A. H. (2016). Self-organization of the in vitro attached human embryo. *Nature* **533**, 251-254.

Donnison, M., Beaton, A., Davey, H. W., Broadhurst, R., L'Huillier, P. and Pfeffer, P. L. (2005). Loss of the extraembryonic ectoderm in Elf5 mutants leads to defects in embryonic patterning. *Development* **132**, 2299-2308.

Dueck, D. and Frey, B. J. (2007). Clustering by passing messages between data points. *Science* **315**, 972-976.

Edgar, R. (2002). Gene Expression Omnibus: NCBI gene expression and hybridization array data repository. *Nucleic Acids Res.* **30**, 207-210.

Faucheux, C., Naye, F., Tréguer, K., Fédou, S., Thiébaud, P. and Thézé, N. (2010). Vestigial like gene family expression in Xenopus: common and divergent features with other vertebrates. *Int. J. Dev. Biol.* **54**, 1375-1382.

Genbacev, O., Donne, M., Kapidzic, M., Gormley, M., Lamb, J., Gilmore, J., Larocque, N., Goldfien, G., Zdravkovic, T., McMaster, M. T. et al. (2011). Establishment of human trophoblast progenitor cell lines from the chorion. *Stem Cells* **29**, 1427-1436.

Hemberger, M., Udayashankar, R., Tesar, P., Moore, H. and Burton, G. J. (2010). ELF5-enforced transcriptional networks define an epigenetically regulated trophoblast stem cell compartment in the human placenta. *Hum. Mol. Genet.* **19**, 2456-2467.

Home, P., Saha, B., Ray, S., Dutta, D., Gunewardena, S., Yoo, B., Pal, A., Vivian, J. L., Larson, M., Petroff, M. et al. (2012). Altered subcellular localization of transcription factor TEAD4 regulates first mammalian cell lineage commitment. *Proc. Natl. Acad. Sci. USA* **109**, 7362-7367.

Horii, M., Li, Y., Wakeland, A. K., Pizzo, D. P., Nelson, K. K., Sabatini, K., Laurent, L. C., Liu, Y. and Parast, M. M. (2016). Human pluripotent stem cells as a model of trophoblast differentiation in both normal development and disease. *Proc. Natl. Acad. Sci. USA* **113**, E3882-E3891.

Jacquemin, P., Hwang, J.-J., Martial, J. A., Dollé, P. and Davidson, I. (1996). A novel family of developmentally regulated mammalian transcription factors containing the TEA/ATTS DNA binding domain. *J. Biol. Chem.* **271**, 21775-21785.

Jacquemin, P., Sapin, V., Alsat, E., Evain-Brion, D., Dollé, P. and Davidson, I. (1998). Differential expression of the TEF family of transcription factors in the murine placenta and during differentiation of primary human trophoblasts in vitro. *Dev. Dyn.* **212**, 423-436.

Knox, K. and Baker, J. C. (2008). Genomic evolution of the placenta using co-option and duplication and divergence. *Genome Res.* **18**, 695-705.

Krendl, C., Shaposhnikov, D., Rishko, V., Ori, C., Ziegenhain, C., Sass, S., Simon, L., Müller, N. S., Straub, T., Brooks, K. E. et al. (2017). GATA2/3-TFAP2A/C transcription factor network couples human pluripotent stem cell differentiation to trophectoderm with repression of pluripotency. *Proc. Natl. Acad. Sci. USA* **114**, E9579-E9588.

Kunath, T., Yamanaka, Y., Detmar, J., MacPhee, D., Caniggia, I., Rossant, J. and Jurisicova, A. (2014). Developmental differences in the expression of FGF receptors between human and mouse embryos. *Placenta* **35**, 1079-1088.

Lee, Y., Kim, K.-R., McKeon, F., Yang, A., Boyd, T. K., Crum, C. P. and Parast, M. M. (2007). A unifying concept of trophoblastic differentiation and malignancy defined by biomarker expression. *Hum. Pathol.* **38**, 1003-1013.

Lee, C. Q. E., Gardner, L., Turco, M., Zhao, N., Murray, M. J., Coleman, N., Rossant, J., Hemberger, M. and Moffett, A. (2016). What is trophoblast? A combination of criteria define human first-trimester trophoblast. *Stem Cell Rep.* **6**, 257-272.

Li, Y., Moretto-Zita, M., Soncin, F., Wakeland, A., Wolfe, L., Leon-Garcia, S., Pandian, R., Pizzo, D., Cui, L., Nazor, K. et al. (2013). BMP4-directed trophoblast differentiation of human embryonic stem cells is mediated through a ΔNp63+ cytotrophoblast stem cell state. *Development* **140**, 3965-3976.

Moretto Zita, M., Soncin, F., Natale, D., Pizzo, D. and Parast, M. (2015). Gene expression profiling reveals a novel regulatory role for Sox21 protein in mouse trophoblast stem cell differentiation. *J. Biol. Chem.* **290**, 30152-30162.

Natale, B. V., Schweitzer, C., Hughes, M., Globisch, M. A., Kotadia, R., Tremblay, E., Vu, P., Cross, J. C. and Natale, D. R. C. (2017). Sca-1 identifies a trophoblast population with multipotent potential in the mid-gestation mouse placenta. *Sci. Rep.* **7**, 5575.

Ng, R. K., Dean, W., Dawson, C., Lucifero, D., Madeja, Z., Reik, W. and Hemberger, M. (2008). Epigenetic restriction of embryonic cell lineage fate by methylation of Elf5. *Nat. Cell Biol.* **10**, 1280-1290.

Niakan, K. K. and Eggan, K. (2013). Analysis of human embryos from zygote to blastocyst reveals distinct gene expression patterns relative to the mouse. *Dev. Biol.* **375**, 54-64.

Nishioka, N., Yamamoto, S., Kiyonari, H., Sato, H., Sawada, A., Ota, M., Nakao, K. and Sasaki, H. (2008). Tead4 is required for specification of trophectoderm in pre-implantation mouse embryos. *Mech. Dev.* **125**, 270-283.

Nishioka, N., Inoue, K.-I., Adachi, K., Kiyonari, H., Ota, M., Ralston, A., Yabuta, N., Hirahara, S., Stephenson, R. O., Ogonuki, N. et al. (2009). The Hippo signaling pathway components Lats and Yap pattern Tead4 activity to distinguish mouse trophectoderm from inner cell mass. *Dev. Cell* **16**, 398-410.

Norwitz, E. R. (2006). Defective implantation and placentation: laying the blueprint for pregnancy complications. *Reprod. Biomed. Online* **13**, 591-599.

Pobbati, A. V., Chan, S. W., Lee, I., Song, H. and Hong, W. (2012). Structural and functional similarity between the Vgll1-TEAD and the YAP-TEAD complexes. *Structure* **20**, 1135-1140.

Rhee, C., Edwards, M., Dang, C., Harris, J., Brown, M., Kim, J. and Tucker, H. O. (2017). ARID3A is required for mammalian placenta development. *Dev. Biol.* **422**, 83-91.

Russ, A. P., Wattler, S., Colledge, W. H., Aparicio, S. A. J. R., Carlton, M. B. L., Pearce, J. J., Barton, S. C., Surani, M. A., Ryan, K., Nehls, M. C. et al. (2000). Eomesodermin is required for mouse trophoblast development and mesoderm formation. *Nature* **404**, 95-99.

Senner, C. E. and Hemberger, M. (2010). Regulation of early trophoblast differentiation - lessons from the mouse. *Placenta* **31**, 944-950.

Shahbazi, M. N., Jedrusik, A., Vuoristo, S., Recher, G., Hupalowska, A., Bolton, V., Fogarty, N. M. E., Campbell, A., Devito, L. G., Ilic, D. et al. (2016). Self-organization of the human embryo in the absence of maternal tissues. *Nat. Cell Biol.* **18**, 700-708.

Shannon, P., Markiel, A., Ozier, O., Baliga, N. S., Wang, J. T., Ramage, D., Amin, N., Schwikowski, B. and Ideker, T. (2003). Cytoscape: a software environment for integrated models of biomolecular interaction networks. *Genome Res.* **13**, 2498-2504.

Soncin, F., Natale, D. and Parast, M. M. (2015). Signaling pathways in mouse and human trophoblast differentiation: a comparative review. *Cell. Mol. Life Sci.* **72**, 1291-1302.

Steegers, E. A. P., Von Dadelszen, P., Duvekot, J. J. and Pijnenborg, R. (2010). Pre-eclampsia. *Lancet* **376**, 631-644.

Strumpf, D., Mao, C.-A., Yamanaka, Y., Ralston, A., Chawengsaksophak, K., Beck, F. and Rossant, J. (2005). Cdx2 is required for correct cell fate specification and differentiation of trophectoderm in the mouse blastocyst. *Development* **132**, 2093-2102.

Supek, F., Bošnjak, M., Škunca, N. and Šmuc, T. (2011). Revigo summarizes and visualizes long lists of gene ontology terms. *PLoS ONE* **6**, e21800.

Tripathi, S., Pohl, M. O., Zhou, Y., Rodriguez-Frandsen, A., Wang, G., Stein, D. A., Moulton, H. M., Dejesus, P., Che, J., Mulder, L. C. F. et al. (2015). Meta- and orthogonal integration of influenza "oMICs" data defines a role for UBR4 in virus budding. *Cell Host Microbe* **18**, 723-735.

Vaudin, P., Delanoue, R., Davidson, I., Silber, J. and Zider, A. (1999). TONDU (TDU), a novel human protein related to the product of vestigial (vg) gene of Drosophila melanogaster interacts with vertebrate TEF factors and substitutes for Vg function in wing formation. *Development* **126**, 4807-4816.

Wakeland, A. K., Soncin, F., Moretto-Zita, M., Chang, C. W., Horii, M., Pizzo, D., Nelson, K. K., Laurent, L. C. and Parast, M. M. et al. (2017). Hypoxia directs human extravillous trophoblast differentiation in a hypoxia-inducible factor-dependent manner. *Am. J. Pathol.* **187**, 767-780.

Yagi, R., Kohn, M. J., Karavanova, I., Kaneko, K. J., Vullhorst, D., DePamphilis, M. L. and Buonanno, A. (2007). Transcription factor TEAD4 specifies the trophectoderm lineage at the beginning of mammalian development. *Development* **134**, 3827-3836.

Zdravkovic, T., Nazor, K. L., Larocque, N., Gormley, M., Donne, M., Hunkapillar, N., Giritharan, G., Bernstein, H. S., Wei, G., Hebrok, M. et al. (2015). Human stem cells from single blastomeres reveal pathways of embryonic or trophoblast fate specification. *Development* **142**, 4010-4025.

DEVELOPMENT